New Method for Estimation of Discharge

Mahmoud F. Maghrebi[1] and James E. Ball[2]

Abstract: A new technique for drawing isovel patterns in an open or closed channel is presented. It is assumed that the velocity at each arbitrary point in the conduit is affected by the hydraulic characteristics of the boundary. While any velocity profile can be applied to the model, a power-law formula is used here. In addition to the isovels patterns, the energy and momentum correction factors (α and β), the ratio of mean to maximum velocity (V/u_{max}), and the position of the maximum velocity are calculated. To examine the results obtained, the model was applied to a pipe with a circular cross section. A comparison between the profiles of the proposed model and the available power-law profile indicated that the two profiles were coincident with each other over the majority of the cross section. Furthermore, the predicted isovels were compared with velocity measurements in the main flow direction obtained along the centerline and lateral direction of a rectangular flume. The estimated discharge, based on measured points on the upper half of the flow depth away from the boundaries was within ±7% of the measured and much better in comparison to the prediction of one- and two-point methods. The prediction of the depth-averaged velocity values for the River Severn in the United Kingdom shows a good agreement with the measured data and the best analytical results obtained by the depth-averaged Navier–Stokes equations.

DOI: 10.1061/(ASCE)0733-9429(2006)132:10(1044)

CE Database subject headings: Open channel flow; Velocity; Discharge measurement.

Introduction

The measurement of the velocity distribution and discharge in a conduit has always been an important issue in hydraulics. While many studies have investigated the vertical velocity profile (Carollo et al. 2002; Lee et al. 2002), little work has been undertaken on isovels in arbitrary shaped channels (Chiu and Tung 2002). From these studies, it is known that the isovel patterns close to a boundary, follow the geometry of the surrounding boundary. However, drawing the isovel contours with an acceptable level of accuracy is a complex task. In fact, the isovel patterns are known only for simple channel geometries. For example, it is known that in a pipe, the isovel pattern is composed of closed circles, with their centers coincident with the pipe centerline. Similarly, in a wide open channel the isovel patterns away from the sides of the channel are known to be parallel to the channel bed. However, even in a simple geometry like a rectangular flume, isovel patterns vary for different aspect ratios.

Practitioners are always searching for suitable means of estimating mean velocity in a variety of channel shapes and sizes with a minimal need for physical measurement. Not only is the current metering often difficult and expensive to carry out, but it also suffers from the fact that a set of the multi-profile, multipoint gaging required for high accuracy cannot easily be carried out quickly enough at times of changing flow characteristics (i.e., depth, velocity), which is common for all natural and some manmade channels. Furthermore, methods that use prescribed positions in the flow to give a fairly good approximation of average velocity (e.g., at $y/d=0.4$ for one point and 0.2 and 0.8 for two-point method where y=distance from bed and d=flow depth) work on the assumption of one-dimensional flow in an infinitely wide channel, which is not always a reasonable premise in the natural channels of nonuniform, unsteady and asymmetrical flow. In "*ideal*" channels, velocity in each grid element in the cross-sectional plane is considered as being controlled by a velocity profile that is affected only by the bed element which is vertically below. Such methods also assume that the bed is horizontal, and that the roughness of adjacent bed element is constant, a situation that occurs practically only in the most carefully constructed (and wide) manmade channels.

A new technique for discharge estimation involves the use of isovel contours in a normalized form to obtain the discharge based on single point of measurement. Referring to Fig. 1, the measured velocity at a point in channel cross section is $u(z,y)$ and the magnitude of the normalized corresponding isovel contour is $U(z,y)$, then the total discharge can be obtained by

$$Q = A\frac{u(z,y)}{U(z,y)} \tag{1}$$

where Q=total discharge passing through the cross sectional area A and $U(z,y)=u(z,y)/V$ with $u(z,y)$ and V as the local point velocity and the mean cross-sectional velocity, respectively. The problem remains of estimating $U(z,y)$ which will be addressed in the rest of the paper.

This paper introduces a new technique for determining the cross-sectional isovels and hence the channel discharge. The use of the developed normalized isovel contours and a single point measurement are required to estimate discharge. The technique is also applicable for unsteady flow situations with small accelera-

[1]Associate Professor, Civil Engineering Dept., Faculty of Engineering, Ferdowsi Univ. of Mashhad, P.O.B. 91775-1111, Mashhad, Iran (corresponding author). E-mail: maghrebi@ferdowsi.um.ac.ir

[2]Associate Professor, Water Research Laboratory, School of Civil and Environmental Engineering, The Univ. of New South Wales, NSW 2093, Australia. E-mail: j.ball@unsw.edu.au

Note. Discussion open until March 1, 2007. Separate discussions must be submitted for individual papers. To extend the closing date by one month, a written request must be filed with the ASCE Managing Editor. The manuscript for this paper was submitted for review and possible publication on November 3, 2003; approved on October 12, 2005. This paper is part of the ***Journal of Hydraulic Engineering***, Vol. 132, No. 10, October 1, 2006. ©ASCE, ISSN 0733-9429/2006/10-1044–1051/$25.00.

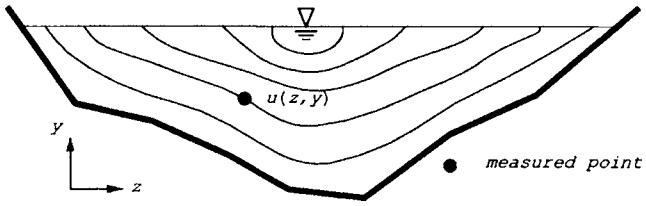

Fig. 1. Single point measurement technique

tion terms, which is the case for large rivers. In large rivers with unsteady flows the flow depth in a channel changes in manner so that multiple velocity measurements at the same flow depth in all verticals become infeasible. However, the model is not expected to handle the flow problems with high acceleration terms.

Velocity Distributions

Any boundary condition that affects the wall shear will alter the distribution of velocity over the cross section; boundary roughness is an example of this feature. The logarithmic velocity distribution for $y > k_s$, is (Yen 2002; Smart et al. 2002; Chen and Chiew 2003)

$$\frac{u}{u_*} = c_1 \ln\left(\frac{y}{k_s}\right) + c_2 \tag{2}$$

where u=local velocity at normal distance y from the wall; c_1 is related to the boundary roughness; c_2=fitting constant; k_s=equivalent Nikuradse sand roughness usually larger than the actual wall roughness height; and $u_* = \sqrt{\tau_0/\rho}$=boundary shear velocity, where τ_0=boundary shear stress and ρ is the mass density of fluid.

The steady uniform turbulent flow of a fluid in a pipe or in an open channel can be expressed by the power-law velocity distribution as (Chen 1991b)

$$\frac{u}{u_*} = c\left(\frac{y}{k_s}\right)^{1/m} \tag{3}$$

A number of investigators have shown the near equivalence of logarithmic velocity law and a one-sixth power law (Brownlie 1983; Wright and Parker 2004).

From Eq. (3), it can be shown that u is proportional to the following factors:

$$\text{(i) } u \propto u_*, \quad \text{(ii) } u \propto y^{1/m}, \quad \text{and (iii) } u \propto (1/k_s)^{1/m} \tag{4}$$

From the first factor, the shear velocity u_* on the bed along the wetted perimeter is proportional to the square root of τ_0. The concept of a constant wall shear stress τ_0 originates from Prandtl's mixing length theory. The boundary shear stress is influenced by the secondary currents and velocity gradients; its distribution over the wetted perimeter of an open channel is known to be nonuniform and depends on the shape of the cross section, nonuniform roughness distribution around the wetted perimeter, and the secondary flow structure (Berlamont et al. 2003; Guo and Julien 2005). The maximum velocity gradient occurs close to the bed and hence the velocity gradient will decrease as distance from the bed increases while the velocity itself increases. Therefore, maximum velocity occurs at the water surface. The value of the power $(1/m)$ varies depending on the intensity of the turbulence. While the value of m typically varies in the range of $4 < m < 12$, a value of 7 is in agreement well with a large number of experimental measurements of turbulent velocity profiles (Chen 1991a; Yen 2002).

The third factor shows that the isovel distribution is affected by the roughness height (k_s) such that u is inversely proportional to a power of k_s. Therefore, as the roughness height increases, the velocity decreases. Although the variation of u_* and k_s, as shown by factors (i) and (iii) in Eq. (4), change the velocity when a uniform shear velocity and/or roughness along the boundary is assumed, the magnitude of these values is not important because the normalized velocity patterns will remain unchanged.

Introduction to Model

The basic idea is derived from the Biot–Savart law in electromagnetics. Then, the similarities between the magnetic field and isovel contours in hydraulics are used to formulate the problem. Let us consider the magnetic field produced by a differential DC element in a free space. It is assumed that a current I is flowing in a differential vector length of filament $d\mathbf{L}$. Then, the law of Biot–Savart states that at any point M, the magnitude of the magnetic field intensity produced by the differential element is proportional to the product of the current, the magnitude of the differential length, and the sine of the angle lying between the filament and a line connecting the filament to the point M where the field is desired. The direction of the magnetic field intensity is normal to the plane containing the differential filament and the line drawn from the filament to the point M (Hayt 1981). The Biot–Savart law may be written using vector notation as

$$d\mathbf{H} = \frac{Id\mathbf{L} \times \mathbf{a}_r}{4\pi r^2} \tag{5}$$

where $\mathbf{H}$=intensity of the magnetic field and $\mathbf{r}$=position vector which connects the element to the considered point M. Now let's consider the boundary of a channel which shows its reach characteristics. The source of isovel contours in the channel section is the boundary. The magnitude of the isovel contour coincided with the boundary is zero. The intensity of the magnetic field of a wire current and the magnitude of the velocity at a cross section due to the boundary are inversely related. At a given point, the closer to the wire, the higher magnitude of the magnetic field whereas in hydraulics the closer to the boundary, the lower the resulting. Referring to Eq. (5), the influence of a finite length of boundary $(d\mathbf{s})$ on the velocity at an arbitrary point is

$$d\mathbf{u} = f(\mathbf{r}) \times cd\mathbf{s} \tag{6}$$

where c=constant related the boundary and $f(\mathbf{r})$=velocity function which is dominant in the flow field. The concept of the line integral is used in both fields. In hydraulics, the velocity in the main flow direction can be obtained by integration along the boundary as

$$u\mathbf{i} = \int_{\text{boundary}} f(\mathbf{r}) \times cd\mathbf{s} \tag{7}$$

It is known the product of $\mathbf{r} \times d\mathbf{s}$=vector normal to the section plane pointing toward downstream with a magnitude of $r\,ds \sin\theta$.

Since vectors $\mathbf{r}$ and $d\mathbf{s}$ are located in a plane normal to the main flow direction, the cross product of them will be normal to the plane of section pointing to the downstream in the streamwise direction. So from Eq. (7) we have

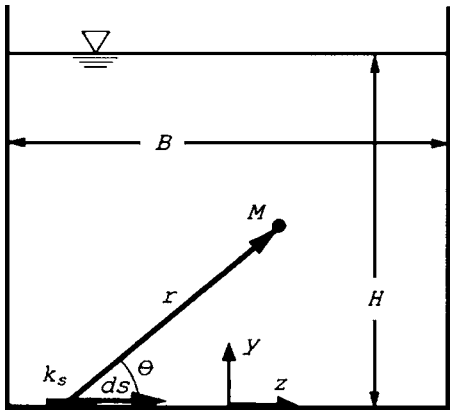

Fig. 2. Illustrative geometry for effect of boundary roughness on velocity of an arbitrary point M in flume

$$u = \int_{\text{boundary}} f(r)c\,ds\,\sin\theta = \int_{\text{boundary}} c\,\sin\theta\,f(r)ds \tag{8}$$

Searching for the best velocity function in terms of r is the next problem. A power law relationship is commonly used to fit velocity profiles in closed conduits and open channels [Eq. (9)]. Eq. (3) can be rewritten as

$$u(z,y) = u_*(c_1 y^{1/m}) \tag{9}$$

where c_1=relative boundary roughness. Assuming the local point velocity at an arbitrary position in the channel section like M in Fig. 2, is a linear function of the influence of the shear along the wetted perimeter, as given by cross product of the positional vector $\mathbf{r}$, and the boundary element $d\mathbf{s}$, we have

$$u(z,y) = \int_P u_*(c_1 r^{1/m})ds \tag{10}$$

The point velocity is subjected to the following restrictions: (1) The velocity distribution within the viscose sublayer will always remain linear; (2) other boundaries cannot influence the velocity within the viscous sublayer; and (3) Due to the no-slip condition, velocity along the wetted perimeter is zero. The local streamwise point velocity is determined by the use of Eq. (6). The average velocity is then given by continuity as

$$V = \frac{\int_A u(z,y)dA}{A} = \frac{\int_A \left[\int_P u_*(c_1 r^{1/m})\sin\theta\,ds\right]dA}{A} \tag{11}$$

The normalized point velocity, $U(z,y)$ is given by the ratio of Eqs. (10) and (11)

$$U(z,y) = \frac{u(z,y)}{V} = \frac{\int_P u_*(c_1 r^{1/m})\sin\theta\,ds}{\frac{1}{A}\int_A \left[\int_P u_*(c_1 r^{1/m})\sin\theta\,ds\right]dA} \tag{12}$$

Assuming constant value for u_*, Eq. (12) will be simplified in finite difference form as

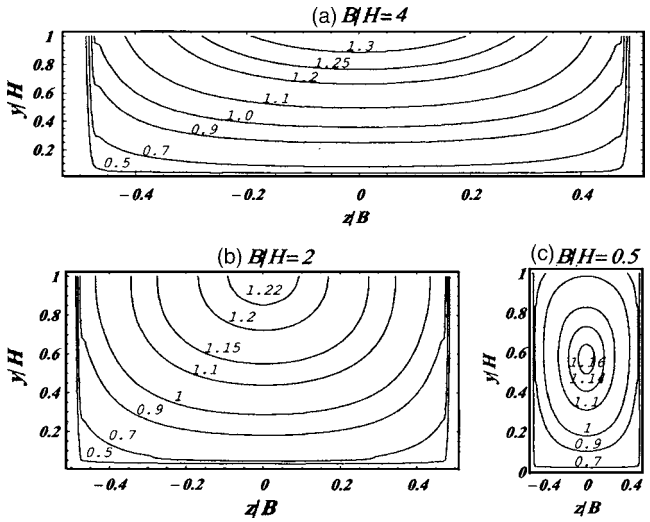

Fig. 3. Isovel contours for different aspect ratios of rectangular flume

$$U(z,y) = \frac{\sum_P c_1 r^{1/m}\sin\theta\,ds}{\frac{1}{A}\sum_A \left(\sum_P c_1 r^{1/m}\sin\theta\,ds\right)dA} \tag{13}$$

where θ=angle between the positional vector and the boundary elemental vector (Fig. 2). Eq. (13) provides the normalized velocity at a point as a simple function of the boundary geometry and relative roughness, c_1. Thus, the average velocity may be obtained from a single measurement $u(z,y)_M$ as

$$V = \frac{u(z,y)_M}{U(z,y)_M} \tag{14}$$

The advantage of the proposed model is that it allows the consideration of the hydraulic characteristics of the boundary and their influence on the flow. To change the boundary conditions such as roughness or shear velocity, it is necessary only to change the relative values of c_1 in Eq. (13). As such, the boundary conditions and the velocity distributions can be altered easily in the model. A description of each factor, which influences the result of isovel pattern, is as follows.

Velocity Profiles

Different velocity profiles can be introduced into the model. For a rough turbulent flow as the usual case in either an open channel or a pipe, there are two well-known velocity distribution functions: the logarithmic profile and the power-law profile. Although the two velocity distributions can be equally used by the model, the power law is used here due to the advantages of simplicity and its algebraic form. The value of the power $(1/m)$ can be changed according to the flow regime and the degree of turbulence in the flow. With increasing Reynolds number R, in smooth pipes, the exponent of the power law expression decreases so the value of m increases as (Hinze 1975)

$$m = 1.825\log(\mathrm{R}) - 1.8 \quad \text{for } 2\times 10^4 < \mathrm{R} < 3\times 10^6 \tag{15}$$

It has been found that a higher exponent of 1/4 can be applied in situation where the roughness is not small scale; e.g., for gravel bed rivers (Smart et al. 2002).

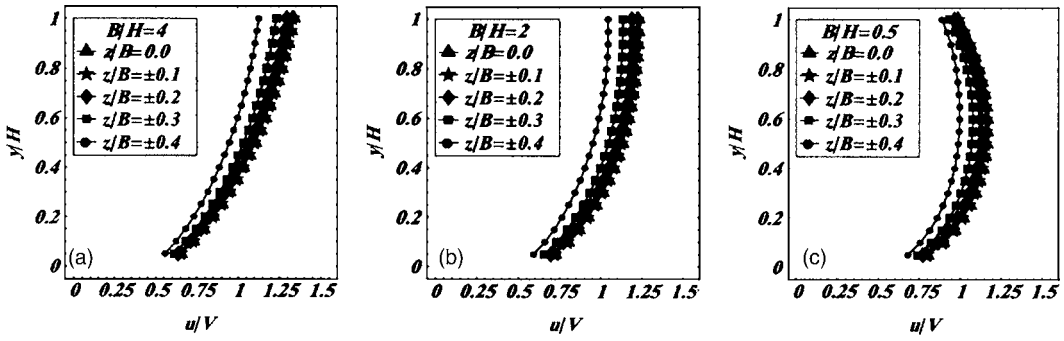

Fig. 4. Velocity profiles for different aspect ratios, corresponding to Fig. 3

Boundary Effects

It is possible to apply different roughness for different boundaries such as the bed and the channel sides. Furthermore, a roughness varying from one position to another—either in a discrete form or in a continuous form with any arbitrary distribution—can be introduced into the model. The asymmetric results of isovels can be obtained from asymmetry of the cross-sectional geometry, bed roughness, and shear stress distributions. However, in this paper, which is applied to a rectangular flume and a river section, the roughness of all boundaries is assumed to be the same.

Application of Model in Rectangular Flume

Fig. 3 shows the isovels for three different ratios of $B/H=4.0, 2.0$, and 0.5, where B and H are shown in Fig. 2. These isovels are calculated using a seventh-root law for the velocity distribution ($m=7$). The values of the normalized isovels $U(=u/V)$, where u is the local velocity in the main flow direction and V is the mean velocity, are given on the contour lines.

A comparison of the isovels in Fig. 3 shows that for larger values of B/H the maximum normalized velocity is considerably larger than smaller values of B/H. It is shown that for a variation of 15 aspect ratios in the range of $B/H=10.0-0.25$, $u_{\max}/V$ varies from 1.45 to 1.15, respectively (Maghrebi 2003). For $B/H=4.0$, it can be seen that the velocity contours are almost parallel to the bed around the centerline of the channel. For values of B/H down to 2.0 the position of the maximum velocity occurs on the centerline at the water surface. As the ratio of B/H decreases the position of maximum velocity goes below the water surface toward the flume center. It is known that the depression of the point of maximum velocity is due to the action of secondary currents in the plane of the channel cross section (Knight et al. 1989). Strong secondary currents are not expected to be formed over a flat plate, whereas close to the corners of a flume such currents are observed. Therefore, it is believed that the geometry configurations are the main source of secondary currents. Although the effect of secondary currents is not considered by the model directly, the effect of geometry is considered by the proposed model. It is obvious that if a solid surface with the same roughness as the other boundaries were defined at the water surface symmetrical isovel patterns would be produced with the maximum velocity at the center of the flume.

The corresponding velocity profiles to Fig. 3 are given in Fig. 4. Velocity profiles for nine different positions at $z/B=0, \pm0.1, \pm0.2, \pm0.3$, and ±0.4 across the channel are plotted in Fig. 4 where z is the distance along bed. It can be seen that for larger aspect ratios the profiles take a more nonuniform shape with the maximum velocity at the top. As the value of B/H decreases, the uniformity of velocity distribution increases with a higher variation of velocity profiles along the flume width at the lower velocity regions close to bed. For deep channels, the maximum velocity deviations along the channel width occur at the central region of the flow.

The coefficient of kinematic energy correction factor, α, and momentum correction factor, β, are calculated by

$$\alpha = \frac{1}{A}\int_A \left(\frac{u}{V}\right)^3 dA \approx \frac{\sum u_i^3 A_i}{AV^3} \tag{16}$$

$$\beta = \frac{1}{A}\int_A \left(\frac{u}{V}\right)^2 dA \approx \frac{\sum u_i^2 A_i}{AV^2} \tag{17}$$

Henderson (1966)and Chadwick and Morfett (1993) indicated that for turbulent flow in regular channels, α and β rarely exceeds 1.15 and 1.05, respectively, which always follow the rule of $\alpha \geq \beta \geq 1$. Additional ranges are presented by Chaudhry (1993) who suggested that for regular channels the ranges of values of α and β are 1.10–1.20 and 1.03–1.07, respectively. However, it should be noted that determination of these factors is hard and needs sufficient number of velocity measurements in a channel cross section. Consequently, in virtually all hydraulic calculations and numerical models of main channel flow, these coefficients have been assumed equal to unity (e.g., Chaudhry 1993). The ratio of mean to maximum velocity $V/u_{\max}$ can be treated as a

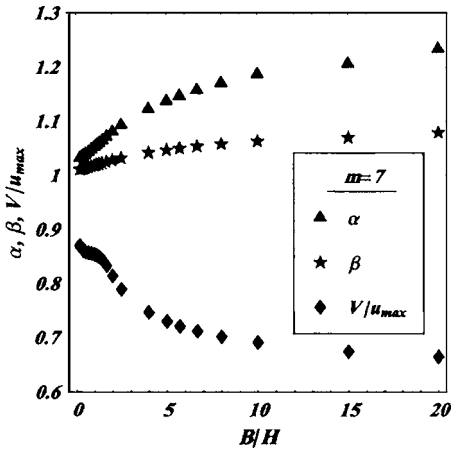

Fig. 5. Calculated values of α, β, and $V/u_{\max}$, in rectangular flume based on seventh-root law

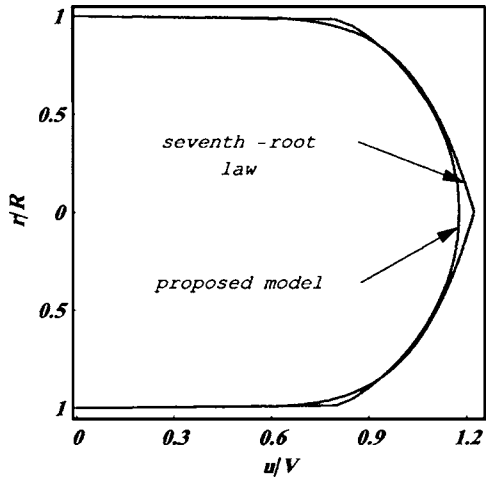

Fig. 6. Velocity profiles in pipe section based on seventh-root law and proposed model with $m=7$

guideline for data collection, and it is useful to understand the hydraulic circumstances of flow either in design or analysis.

In Fig. 5 variations of α and β as well as V/u_{max}, with respect to B/H are shown. As it can be seen, when B/H increases, α and β increase due to the increase of nonuniform velocity distribution. The results are in good agreement with the suggested values of α and β for regular channels (Chaudhry 1993). Also, as B/H increases, V/u_{max} decreases and for a very wide open channel it approaches 0.65.

When B/H decreases for a deep and narrow channel, the uniformity of velocity distribution increases, meanwhile V/u_{max} approaches a value of 0.9. These are in accordance with the power law velocity distribution and also in agreement with the results reported by Chiu and Tung (2002).

In order to validate the values of α and β we have applied the model to a circular pipe with full flow. The theoretical values of these parameters are available. In pipes with a circular section the shear stress restraining the fluid motion is uniformly distributed around the boundary of the cross section and the effects of secondary currents are distributed uniformly over the cross section. For a turbulent flow in a pipe with a velocity distribution of seventh-root law $\alpha=1.058, \beta=1.020$, and $V/u_{max}=0.817$. The calculated results based on the proposed approach are: $\alpha=1.040$; $\beta=1.013$; and $V/u_{max}=0.848$.

The result of velocity profile for a pipe section in a dimensionless form is given in Fig. 6. The mean velocity occurs at $r/R=0.74$, while the seventh-root law gives its value at $r/R=0.758$. Except at very close to the wall and the center of pipe, where some differences between the profiles of the proposed model and the seventh-root law can be observed, on most parts of the pipe section the two velocity profiles are extremely close to each other. Actually, the power-law formula, which produces a discontinuity in the velocity profile slope at the center of the pipe, is obviously unrealistic at the central part of the pipe. The proposed model has produced a velocity profile without this discontinuity. It is observed that the main reason for the difference between the values of α and β is due to this area.

Experimental Works and Results

The experiments were conducted in a tilting flume. The flume was 8.0 m long, 0.25 m wide, and 0.29 m high with bed and walls made from glass. Discharge was measured with carefully calibrated orifice plates located in the supply pipe. The location of the test section was located 5.5 m from the upstream entrance of the flume. The experiments were carried out for three flow depths of 0.15, 0.20, and 0.25 m, which correspond to $B/H=1.67, 1.25$, and 1.0, respectively. For the first set of experiments, the velocity profiles were measured along the centerline of the flume with a gap of 2 cm in a vertical direction almost up to the water surface. A miniature propeller with a diameter of 1 cm was used to measure the time-averaged velocity u for a duration of 120 s.

Since the measured mean velocity is different from the calculated mean velocity, even if a solid circle of measured velocity is located on the profile of the proposed model, it does not mean that a perfect agreement between the measured and calculated velocities exists. However, if the measured velocity profile follows the calculated profile with a horizontal gap, it guarantees almost a constant difference between measured and calculated velocities and in turn the discharges (see Fig. 7).

Having a point of measured velocity anywhere in a flume section and using the isovel contour lines given in Fig. 3, one can easily obtain the discharge, which is called the calculated discharge based on the proposed model. On the other hand, the measured discharge for each case of aspect ratio is available. The relative percentage of error in discharge estimation is calculated

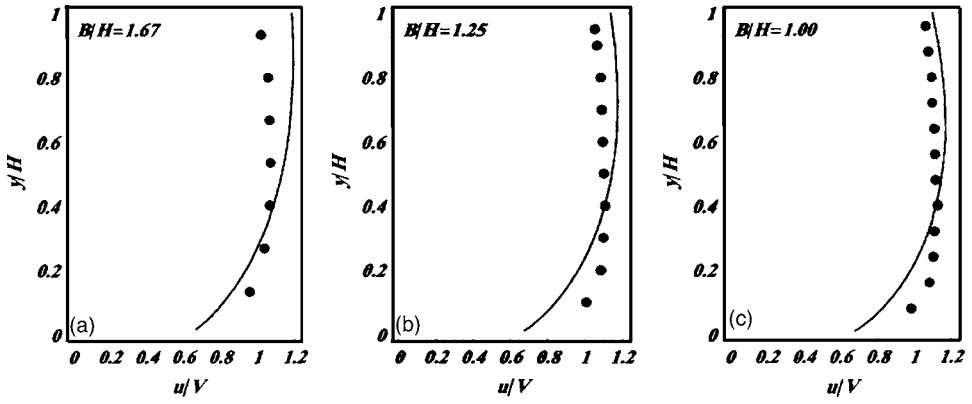

Fig. 7. Comparison of measured data along centerline of flume flow with profile of proposed model: (a) $B/H=1.67$; (b) $B/H=1.25$; and (c) $B/H=1.00$

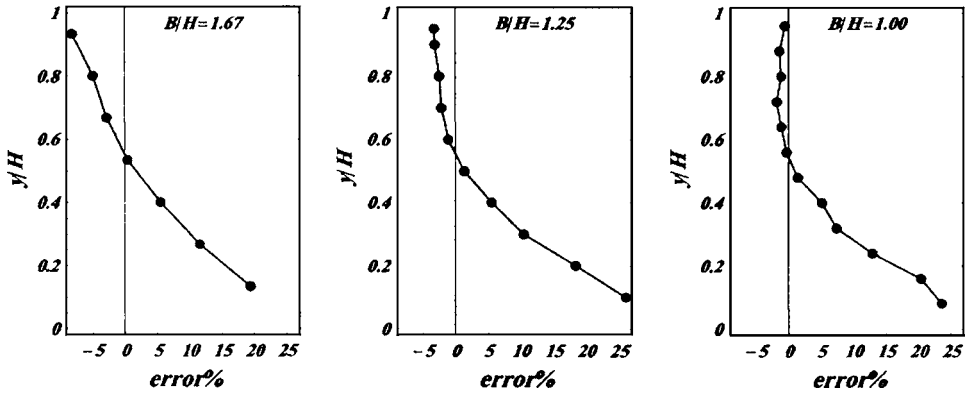

Fig. 8. Percentage of error in discharge assessment using one point of measurement along centerline, corresponding to Fig. 7

by error $\% = [(Q_c - Q_m)/Q_m] \times 100$, where Q_c and Q_m = calculated and measured discharges, respectively.

Figs. 8(a–c) show the percentage of error for each point of measurement corresponding to Figs. 7(a–c). It can be seen that if the measured points close to bed are used for discharge estimation, a larger error occurs as compared to using measurements closer to the water surface. With increasing elevation toward the water surface, the error decreases. If the one- and two-point methods are used to estimate the discharge based on the measured points, a much larger error will be observed. The results are given in Table 1. It should be noted that for all three cases, the two-point method in comparison with the one-point method provides a lower error in the discharge estimation. The trends of error in discharge assessment, as presented in Figs. 8(a–c), are generally true because at the lower parts of channel, lower values of isovel contour are observed. Therefore, when the actual discharge is calculated, a small difference in the velocity measurement can lead to a large error in the discharge estimation. In other words, as previously mentioned, the computed mean velocity can be obtained by $u(z,y)/U(z,y)$, where $u(z,y)$ is the measured velocity and $U(z,y)$ is the value of isovel associated with the location of the measured point. Calculations based on lower values of $U(z,y)$ lead to a higher value of errors.

In the second set of experimental works, velocity measurements have been carried out along a horizontal line at $y/H=0.8$ for different aspect ratios of $B/H=4.0, 2.0$, and 1.0. Velocity measurements were conducted at $z/B=0, \pm 0.1, \pm 0.2, \pm 0.3, \pm 0.4$, and ± 0.45. The results of measurement and the horizontal velocity profiles extracted from the data of the proposed model are shown in Fig. 9. In this figure the solid circles of the measured velocities are compared with horizontal velocity profile at $y/H=0.8$ for the corresponding aspect ratios. The figure shows a good agreement between these two; however close to the wall a larger deviation between the measured points and the velocity profiles can be observed. The corresponded errors of discharge estimation are located in the range of $\pm 5\%$. Expectedly, the errors corresponded to the measured point at $z/B = \pm 0.45$ for $B/H=1.0$ reach 12.5%. They are not shown here.

Application of Model to River

Application of the proposed model to a natural river is examined. Babaeyan-Koopaei et al. (2002) have reported the velocity and turbulent measurements in the River Severn (U.K.). The mean characteristics of the river flow are given as $Q=103\ m^3/s$, $V=0.7$ m/s, with $R=1.813\times 10^6$. The measured section of the river was located at a single meander of about 600 m long. Velocity measurements of the cross section were carried out using a directional current meter (DCM) at different depths of the flow for each lateral direction to an accuracy of 0.1 m/s. Then the depth-averaged velocity values u_d were obtained along the lateral direction. The results are shown in Fig. 10.

In an attempt to compare the predicted results of the model with the measurement data, the model has been used to obtain the depth-averaged velocity values for the same section of the River Severn. Determination of the roughness heights in natural rivers is a laborious task. This not only depends on the size of material at the considered local point but also on the variation of the roughness along the section and the upstream reach. Thus, the roughness of the channel boundary over the entire cross section is assumed to be uniform. Although the sensitivity of the results predicted by the proposed model is not high with the variation of exponent $1/m$, a sixth-root law which is more consistent with a turbulent rough flow in rivers with a relatively large roughness element, is used in the model. The best analytical solution of the depth-averaged Navier–Stokes equations including the secondary current term obtained by Ervine et al. (2000) at the same cross section of the river is also shown in Fig. 10. Although the predicted results of the model over the flood plain is a little lower than the measured data, overall a good agreement among the measured, analytical, and the predicted depth-averaged velocity values can be observed.

Conclusions

A new analytical technique for drawing the isovel contours quantitatively in a conduit with an arbitrary-cross-sectional shape and boundary roughness has been presented. The simplicity of the model can be considered as one of its major advantages as compared with other analytical and numerical methods. Other com-

Table 1. Error for Estimation of Discharge Using One- and Two-Point Methods

Aspect ratio B/H	One-point method (%)	Two-point method (%)
1.67	+14.97	+10.64
1.25	+16.96	+14.47
1.00	+17.79	+14.26

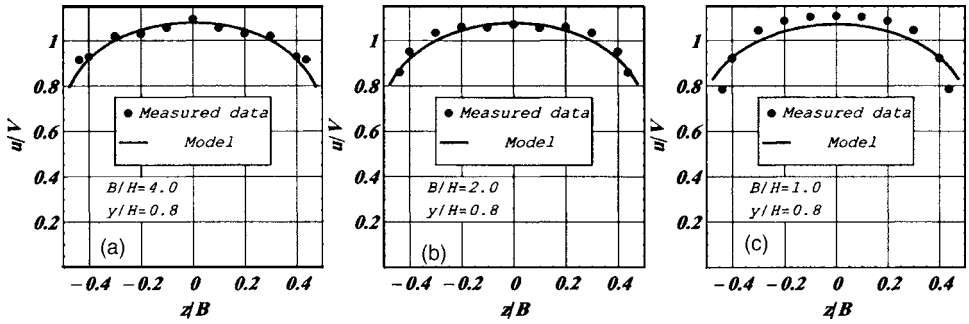

Fig. 9. Comparison of measured data along centerline of flume flow with profile of proposed model: (a) $B/H=4.0$; (b) $B/H=2.0$; and (c) $B/H=1.0$

plicated models are engaged with several simplifying assumptions and relatively a large number of calibrating parameters. The result of the model when applied to a pipe flow shows that except for points very close to the boundary, the rest of velocity profile coincides with the profile of the introduced velocity with an exception at the central region of the pipe flow. As a result, the velocity profile obtained for pipe seems to be more realistic as compared to the regular velocity profiles such as power-law formula.

In the single point measurement technique proposed herein, the estimated discharge when compared to the measured discharge shows that if the measured points are selected from the upper half of the water depth and away from the boundaries, the estimated discharges are much closer to the measured discharge. For a larger range of aspect ratios between $B/H=4.0$ and 1.0, when the measured points are selected at $y/H=0.8$, the percentage of error in discharge estimation is low and it does not depend much on the lateral positions of the measured points except close to the walls. The model prediction shows a good agreement with the measured data. Furthermore, application of the model to a section of the River Severn shows a good prediction of depth-averaged velocity when compared with the best results of analytical solutions of the Navier–Stokes equation and measured values.

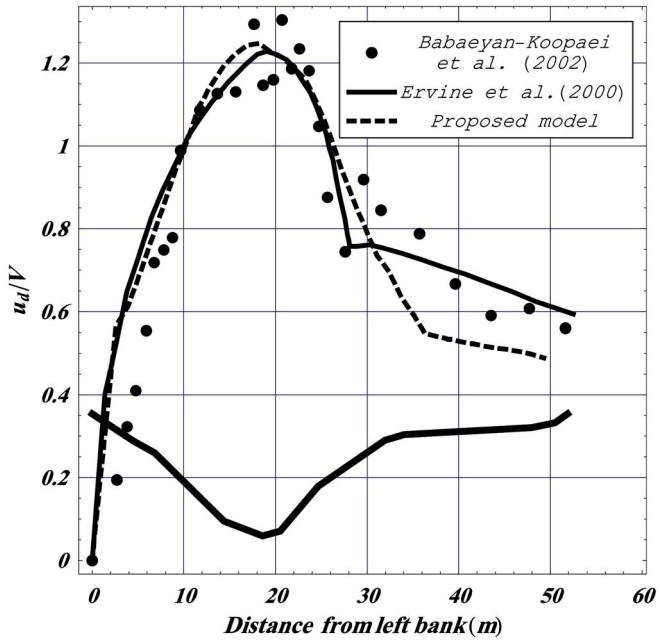

Fig. 10. Predicted depth-averaged velocity by proposed model against best analytical as well as measured values in River Severn (March 2000)

Notation

The following symbols are used in this paper:

A = area of flow;
B = flume width;
c, c_1, c_2 = constants;
D = diameter of circular section;
d = flow depth;
dL = finite element of current wire;
ds = finite element of boundary;
g = gravity acceleration;
$\mathbf{H}$ = intensity vector of magnetic field;
H = flume depth;
I = current intensity;
$\mathbf{i}$ = unit vector in streamwise direction x;
k_s = Nikuradse's equivalent sand roughness;
m = denominator in exponent of power law velocity distribution;
Q = discharge;
Q_c = calculated discharge;
Q_m = measured discharge;
R = Reynolds number;
R = radius of circular section;
r = radial distance;
U = normalized flow velocity;
u = streamwise flow velocity;
u_d = depth-averaged velocity;
$u_{\max}$ = maximum velocity;
u_* = shear velocity;
V = average velocity of flow;
y = distance from boundary;
z = distance measured in lateral direction;
α = kinematic energy correction factor;
β = momentum correction factor;
μ = dynamic viscosity of fluid;
ρ = density of fluid; and
τ_0 = bed shear stress.

References

Babaeyan-Koopai, K., Ervine, D. A., Carling, P. A., and Cao, Z. (2002). "Velocity and turbulence measurements for two overbank flow events in River Severn." *J. Hydraul. Eng.*, 128(10), 697–705.

Berlamont, J. E., Trouw, K., and Luyckx, G. (2003). "Shear stress distribution in partially filled pipes." *J. Hydraul. Eng.*, 129(9), 891–900.

Brownlie, W. (1983). "Flow depth in sand-bed channels." *J. Hydraul. Eng.*, 109(7), 959–990.

Carollo, F. G., Ferro, V., and Termini, D. (2002). "Flow velocity measurements in vegetated channels." *J. Hydraul. Eng.*, 128(7), 669–673.

Chadwick, A. J., and Morfett, J. C. (1993). *Hydraulics in civil and environmental engineering*, Chapman and Hall, London.

Chaudhry, M. H. (1993). *Open-channel flow*, Prentice–Hall, Englewood Cliffs, N.J.

Chen, C. L. (1991a). "Power-law of flow resistance in open channel: Manning formula revisited." *Centennial of Manning's formula*, Water Research, Charlottesville, Va., 206–240.

Chen, C. L. (1991b). "Unified theory on power laws for flow resistance." *J. Hydraul. Eng.*, 117(3), 371–389.

Chen, X., and Chiew, Y. M. (2003). "Response of velocity and turbulence to sudden change of bed roughness in open-channel flow." *J. Hydraul. Eng.*, 129(1), 35–43.

Chiu, C. L., and Tung, N. C. (2002). "Maximum velocity and regularities in open-channel flow." *J. Hydraul. Eng.*, 128(4), 390–398.

Ervine, D. A., Babaeyan-Koopai, K., and Sellin, R. H. J. (2000). "Two-dimensional solution for straight and meandering overbank flows." *J. Hydraul. Eng.*, 126(9), 653–669.

Guo, J., and Julien, P. Y. (2005). "Shear stress in smooth rectangular open channel flows." *J. Hydraul. Eng.*, 131(1), 30–37.

Hayt, W. H. (1981). *Engineering electromagnetics*, 4th Ed., McGraw–Hill, New York.

Henderson, F. M. (1966). *Open channel hydraulics*, Macmillan, New York.

Hinze, J. O. (1975). *Turbulence*, McGraw–Hill, New York.

Knight, D. W., Shiono, K., and Pirt, J. (1989). "Prediction of depth mean velocity and discharge in natural rivers with overbank flow." *Proc., Int. Conf. on Hydraulics and Environmental Modeling of Coastline, Estuaries and River Waters*, Univ. of Bradford, Sep. Gower, Aldershot, U.K., 419–428.

Lee, M. C., Lai, C. J., Leu, J. M., Plant, W. J., Keller, W. C., and Hayes, K. (2002). "Noncontact flood discharge measurements using an X-band pulse radar (I) theory." *Flow Meas. Instrum.*, 13, 265–270.

Maghrebi, M. F. (2003). "Discharge estimation in flumes using a new technique for the production of isovel contours." *Proc., Int. Conf. on Civil and Environmental. Engineering*, ICCEE, Hiroshima, Japan, 147–156.

Smart, G. M., Duncan, M. J., and Walsh, J. M. (2002). "Relatively rough flow resistance equations." *J. Hydraul. Eng.*, 128(6), 568–578.

Wright, S., and Parker, G. (2004). "Density stratification effects in sandbed rivers." *J. Hydraul. Eng.*, 130(8), 783–795.

Yen, B. C. (2002). "Open channel flow resistance." *J. Hydraul. Eng.*, 128(1), 20–39.